ThermoFlowScan: Automatic Thermal Flow Analysis of Machines from Infrared Video

Arindam Saha, Jitender Maurya, Sushovan Mukherjee and Ranjan Dasgupta

Embedded Systems and Robotics, TCS Research & Innovation, Kolkata, India
{ari.saha, jitender.maurya, sushovan.mukherjee, ranjan.dasgupta}@tcs.com

Keywords: Infrared Image, Segmentation, Feature Extraction, Thermal Flow Measurement, Machine Condition Monitoring.

Abstract: Periodic maintenance is a primitive task for preventive maintenance of machines. Abnormal heat generation or heat flow is one of initial indicators of probable future failure. In this paper we presented an autonomous inspection system for heat flow monitoring and measurement of machines in non-invasive way. The proposed system uses infrared (IR) imaging to capture thermal properties of machines that generate heat. Heat sources are segmented and all segmented regions are tracked until heat is present to record the changes in heat pattern. Every hot segment is broken into multiple buckets that aligned towards a specific direction. Heat propagation towards every direction is analysed. The outcome of the presented analysis calculates rate of thermal flow along every directions. Presented results show that the proposed method is capable of measuring heat flow accurately for different type of machines and the analysis has usability in the domain of predictive maintenance for machines.

1 INTRODUCTION

Primary goal of a machine manufacturer is to produce machines that deliver output consistently within a specified error tolerance. Low tolerant machines are required to have high level of repeatability and accuracy. There are many sources of error responsible for affecting these machine performance parameters and abnormal heat generation or heat flow is initial indicators of such errors. Periodic maintenance is one of primitive task for preventive maintenance. The inspection is a sensitive work in many other industries like oil refineries, manufacturing, mechanical and it is carried out in offline mode and industries faces a downtime loss for offline inspection. Machine condition monitoring is done for the use of predictive maintenance, which is not only determining present systems, but it is a technology of predicting future possible abnormalities. The need of continuous unobtrusive machine inspection is gaining popularities during recent years for cost savings. The main goal of automatic machine maintenance in an unobtrusive way is to health checking of industrial machines to reduce down time cost to industries. Maintenance work usually is done on the basis of some parameter which gives information about machine conditions like temperature, vibrations, pressure, flow etc. In this paper
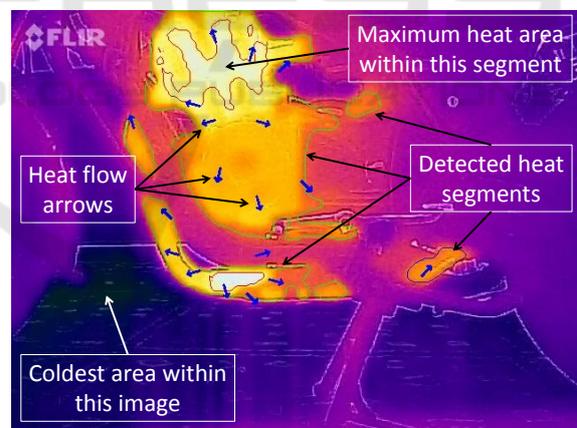

Figure 1: Thermal Image: Multi-level segmentation of heated regions with heat flow directions.

we are focusing on continuous assessment of thermal profile of machines.

Abnormal heat generation and thermal flows in any machine are early signs of any fault. Abnormal temperature rise in a machine can cause damage to several components in the system resulting in down time and high repair costs. It is crucial to avoid abnormal heat generation and flow for increase machines longevity. With the above motivation, we present an end to end computationally inexpensive

637

system to monitor thermal condition of machines using IR imaging and machine vision. Proposed system is capable of detecting sudden heat changes and autonomous heat flow by analysing thermal contour behaviour or heat distribution profile. Major contributions for the presented work are:

- All heat sources are detected, segmented, tracked through out the inspection duration.

- Rate of heat flow on all directions for every heat source are calculated.

- Presented system is computationally inexpensive and performs in real-time.

2 LITERATURE REVIEW

Several studies are available on finding thermal changes on infrared images. The studies are focused several areas like diagnosing disease on human bodies, monitoring building power consumption, monitoring factory manufactured product etc. Heat signature changes with disease either on the skin or inside muscular tissue. So researchers showed interest on finding early symptoms of many diseases by analysing the heat signature of human body (Kaczmarek and Ruminski, 2009; Bagavathiappan et al., 2009). Recently Rajoub & Zwiggelaar (Rajoub and Zwiggelaar, 2014) proposed facial thermal analysis for deception detection. These methods are limited to check small heat changes from a single image and are not suitable to measure heat flow on machines.

Building interior monitoring is another major usage of thermal imaging. Researchers proposed several methods for 3D thermal mapping for build monitoring (Vidas et al., 2013; Omar et al., 2014). Usages of optical and infrared cameras are gaining interest for creation of 3D thermal model (Rangel et al., 2014; Saha et al., 2016). Thermal profile shows any heated object very distinctly in the scene and this feature help detection of any animal in dark. Researchers (Weinmann et al., 2014; Pal et al., 2016; Deshpande et al., 2015) showed methods for object detection through thermal imaging on robotic platform. All methods detect heated object without any proposition for thermal flow measurement.

Starman & Matz (Starman and Matz, 2011) presented a system for detecting cracks using infrared thermography. This proposed system is very costly and very specific to object. So the usages are limited for easy general usage for industrial predictive analysis. Clough et al. (Clough et al., 2012) proposed methods for condition monitoring thermal error for spindles through thermal imaging. The system is limited to only continuous temperature monitoring of different parts of spindle. Al-Habaibeh & Robert (Al-Habaibeh and Robert, 2003) proposed a method for an autonomous monitoring system for several manufacturing like drilling, grinding, welding etc. using novelty detection. Both the methods are lacking in analysis of heat flow which is the most important feature for predictive machine inspection. Eftekhari et al. (Eftekhari et al., 2013) proposed a fault detection algorithm for circuit fault in the stator windings of an induction motor. The process generates histogram of temperature profile. It also explores the correlation between hottest region on the motor body and the fault severity. Subsequently, a comparison is made with healthy motor features. Proposed method is very much limited with the type of the machine and required generalization for usage in a wide range of machines. Ashish & Vijay (ASHISH and VIJAY, 2014) presented a survey for fault detection of machines based on temperature where standard deviation, mean, skewness, energy, entropy are calculated on the entire image to understand fault. So these systems are limited to find out any sudden abnormal heat immediately.

3 SYSTEM OVERVIEW

Conditional monitoring is the process of identifying a significant change which is indicative of a developing future fault in machines. Our goal is to present a heat flow analysis model which will help us understand further, such indicative behaviour of machines in an unobtrusive way. Heat profile of any machines changes with time and it flows from heat source to colder regions, results in continuous heated regions. We assume a machine would generate unwanted heat patterns and flows in case of any fault. Therefore we keep our interest only on finding heated regions and corresponding heat flows.

3.1 FLIR based Infrared Imaging

Thermal imaging device or infrared cameras, can only detect radiated heat energy. FLIR produces different variety of infrared imaging devices which is customized for specific type usage. FLIR recently launched a very cost effective product called FLIR ONE (http://www.flir.com.hk/flirone), a smart-phone attachment for easy usage by everyone. Our proposed system uses a FLIR ONE as infrared imaging device. FLIR ONE thermal sensor comes with 160x120 thermal resolution and optical sensor with 640x480 resolution. Both images are blended using FLIR MSX

technology and final resolution is 640x480. FLIR ONE is capable to detect temperatures between -20 degree Celsius to 120 degree Celsius with a resolution of 0.1 degree Celsius and captures thermal videos with a speed of 6 fps approximately. Frames are stored in 4:2:0 YUV format and encoded with h264 encoder.

3.2 Colour Palettes

Thermal cameras operate on infrared range which is way beyond the range of visible light. Instead of directly detecting color, by means of a two-step process, the camera first records thermal information and subsequently, the thermal information is displayed in the form of an image such that it is amenable to visual interpretation. Images are represented using a false color representing the difference in temperature to easily analyse a thermal image visually. Iron palette is the most commonly used color palette with the coldest and hottest areas being connoted as black and white respectively. In the said palate, blue and purple indicate slightly hotter areas, whereas mid-range temperatures are represented as red, orange and yellow. A sample image is shown in Fig. 1. Owing to the relative nature of the presentation, a color does not map to a particular temperature. Thus, in two different image, the same color may represent two different temperature. e.g. black on a thermal image may represent 0 degree Celsius whereas on another, it may represent 25 degree Celsius. The significance of the colors only implies a relative separation of hotter or colder region, allowing one to easily distinguish between hottest and coldest parts. Recorded videos using FLIR ONE provides only color annotated images of heat.

3.3 Software Architecture

We have exploited several features of FLIR ONE into our proposed method. The proposed system block diagram is shown in Fig. 2. FLIR ONE is placed in front of machines under inspection and thermal videos are captured using smart-phone application. The video recording is continued until the heat is visible on the screen after powering off the machine. Hotter regions are segmented out. Flow of heat for every region is analysed throughout the captured video duration. Each hot segment is broken into multiple buckets such that each bucket is aligned towards a particular direction. Total number of buckets would depend on corresponding contour shape and size. The analogy is to keep the total number of buckets as high as possible but with a minimum length of perimeter
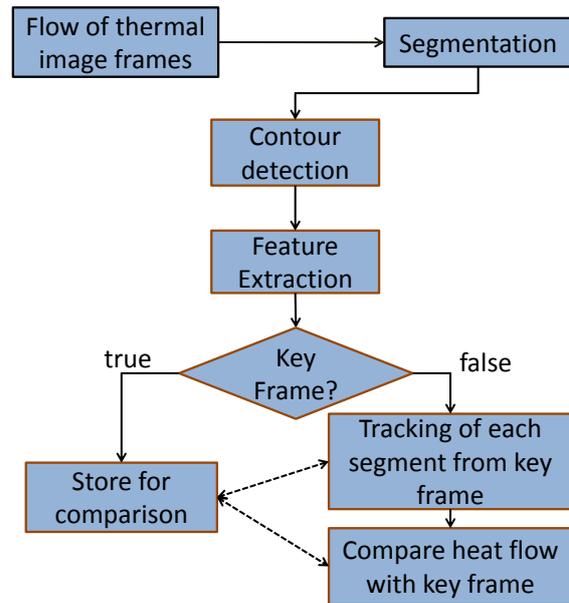

Figure 2: System Flow Diagram.

to identify any small changes in contour towards any direction. Bucketing method is explained in Sec. 4.3. The change in heat flow is governed by law of physics and thus spreads in heated segments are not random. This phenomenon motivated us to use combination of perimeter and area towards a small range of directions (for one bucket) to find out changes in shape of heated regions though perimeter and area are independently non-invariant features of shape. There are possibilities where perimeter or area fails to detect any changes but such cases would not occur due to nature of heat flow. Features are tracked and compared throughout entire captured duration to measure thermal flow. The change in heat flow is governed by second law of Thermodynamics and our experimental results could not found much difference in heat flow between two consecutive frames when we capture video even with very low frame rates like near to 6 fps. Therefore the comparison and measurement are executed based on key frames which are considered after some intervals. Intensity is another feature that helps to identify uniform heat increase without contour changes.

4 FEATURES

Frames are decoded and processed in a sequential way. Iron color palette is used to represent hotter and colder areas of an image as described above and storage format is in three channel colour format (RGB). Temperature is a single channel quantity represented

with three channel pseudo colour format for better visual impact on human eyes. Therefore separation between hot and cold regions must be decided by chroma and luminance should have very little effect. HSV (Hue, Saturation and Value) is the representation where chroma is mapped into single channel called hue. HSV color representation is used for segmentation. RGB to HSV conversion is performed as described by Alvy (Alvy, 1978).

We defined combinational features for every segment for unique identification, result in stable tracking of each segment with accurate flow calculation. Features are extracted on the gray scale image. Conversion to gray scale is achieved by Eq. (1) (Rafael and Richard, 2006).

$$Y = 0.299R + 0.587G + 0.114B \qquad (1)$$

Where Y = gray intensity value and R, G, B represents the red, green and blue channel intensity values respectively.

Heat source is the hottest region in a segment. Therefore hottest point in a segment would not change very fast due to the nature of heat flow. This motivates us to use the hottest point or local maxima to track region of interest (ROI). Perimeter and area towards every bucket help to measure heat flow direction as already mentioned in Sec.3.3. Average intensity helps to identify uniform heat increase even without contour changes.

4.1 Segmentation

Segmentation, in the parlance of image processing, is the process of separating a digital image into multiple segments (contiguous group of pixels) and represents the image in a way that is more meaningful and easier to analyse. Heated areas in a thermal image are of our ROI's and segmentation is used to segregate out hot areas. Every hot segment in a thermal image is having temperature distribution due to heat flow resulting changes of color gradually. Therefore a single segment is not every time suitable to represent a bigger heated region. Multiple level of segmentation is used for such kind of scenario which generates multiple contours within one contour to segregate multiple level of heated segments. Selected hue and saturation ranges from HSV representation are used for segmentation. Value field is ignored because it is assigned the max value from RGB channel as described in the algorithm. The effect of discarding values on HSV planes is experimentally verified. Brightness of a thermal image is varied within a range of -70 to +70 which eventually change the value field on HSV
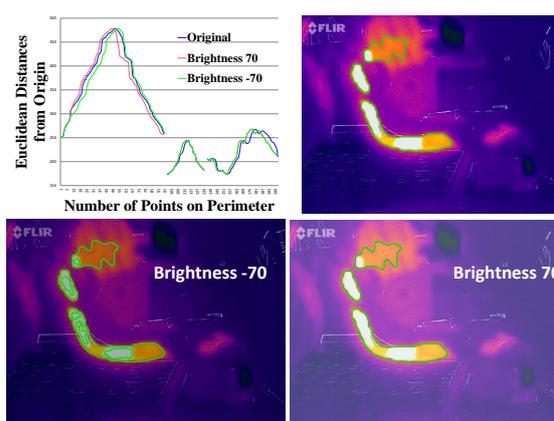

Figure 3: Segmentation with varying brightness and saturation.

plane. Segmentation process shows almost non invariant to the change of value. The graph in Fig. 3 represents Euclidean distances of points lies on the contours with different values of brightness and images shows the detected segments. The overlapping curves represent similar segmented contour shapes.

Particular color segment are chosen based on the color representation on thermal images. The selected color segment is represented on the Fig. 4. The selected color segment is used as threshold parameters for hot area segmentation. Multilevel segmentation uses multiple threshold parameters from hue and saturation selection. Two level segmentation is shown Fig. 1.

It is interesting to note that, driven by the relative scale in temperature presentation, while significant heating up occurs in the system the coldest zone in the frame (likely to be far outside the actual system concerned) turns darker. This can be seen, e.g. between the transition from the frame with time tag of '18.667 sec' and '1 min 39 sec' in Fig. 6. Governed by the physical reasoning that the coldest zone, away from any proximal heat transfer effect of the sources, does not undergo significant temperature change, hence, may serve as a mechanism to counter the relativity effect in color depiction. So, we can benchmark against the coldest zone and can accordingly modify the thermal contour for better segmentation.

Segmentation produces heated regions which are our ROI. Satoshi & KeiichiA (Satoshi and KeiichiA, 1985) presented contour detection algorithm using topological structural analysis of digitized binary images by border following, we make use of same method to detect contour of all ROIs.
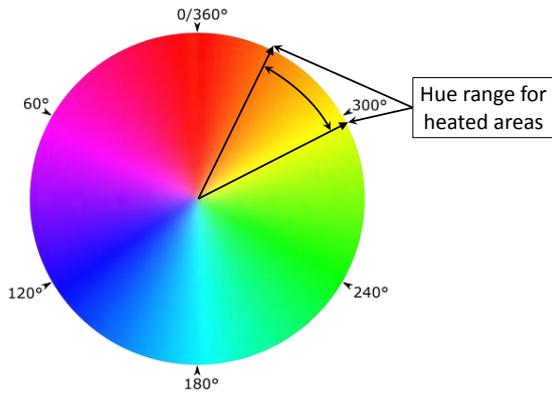
Figure 4: Hue range for thermal segmentation on HSV palne.

4.2 Tracking

Heat flow measurement requires tracking heated regions for long duration. Tracking requires unique identification of every heated region for entire inspection duration which is quite long in case of steady heat growth and decay. Local maximum heat point in every segment is used for tracking corresponding segment for entire inspection duration. Many time heats are spread in a way that there exists a small region which represents most heat instead of a single point. The most heat region is basically the heat source which does not changes rapidly. We exploit this phenomenon for tracking a segment. Centroid of most heat region is used in tracking. Centroid is defined as the pixel with average coordinate values of pixels on perimeter of mostly heated region inside one segment. So this pixel can be treated as local maxima. Centroid calculation follows Equ. 2.

$$C_x = \frac{\sum_{x=1}^{n} P_x}{n}, C_y = \frac{\sum_{x=1}^{n} P_y}{n} \qquad (2)$$

Where P is a point on perimeter with x, y coordinates are P_x, P_y and n is the total number of points on perimeter.

Centroids are tracked through the calculation of minimum Euclidean distances from previous key frame (shown in Algo. 1). One advantage of tracking through centroid is centroids of local maxima do not move much between two successive key frames, results robust tracking.

Algorithm 1: Tracking of Heat segments.

1: **procedure** TRACK
2:    *loop*: [for all Centroid (C) $\in$ current frame]
3:    Find Min(C, C$_{key}$) [for all Centroid (C$_{key}$) $\in$ key frame]
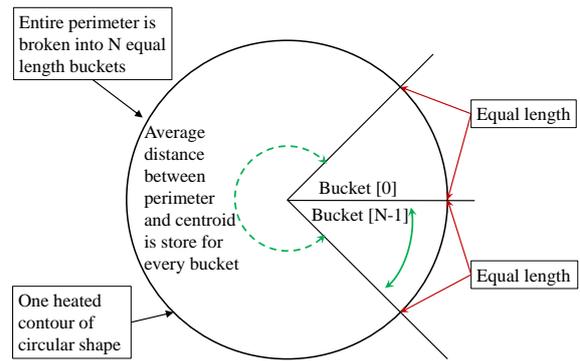4:   *end loop*

Figure 5: Bucket formation.

Area, perimeter and average intensity are calculated for every segment. Area is defined as number of pixels inside of a segmented region. Perimeter is defined as total number of pixels on a contour of any segmented area. Average intensity is the average gray value of pixels within one segment and calculated using Equ. 3.

$$I_{avg} = \frac{\sum_{p=1}^{m} I_p}{m} \qquad (3)$$

Where I_p denotes the gray intensity of point p $\in$ m where m is total number of points inside the segment.

4.3 Bucket Formation

Heat flow measurement requires identification of directions where heat spread either increment or decrement. These directions are infinite theoretically, but feasible implementation requires directions to be in finite numbers. Therefore directions are calculated by dividing entire perimeter of a segmented area into multiple numbers of directions called buckets. Perimeter is divided into small angles and stored in each bucket. Angles and Euclidean distances from centroid are calculated for each perimeter point belongs to a bucket. The average Euclidean distance will represents present heat status of that bucket. This calculation is repeated for every bucket of all segments. A bucket is broken into multiple buckets when perimeter of corresponding bucket will grow with heat spread. Bucket formation is shown visually on Fig. 5.

Signature for every ROI is defined with area, perimeter, centroid of most heated region (local maxima), bucketing and average intensity for unique identification.
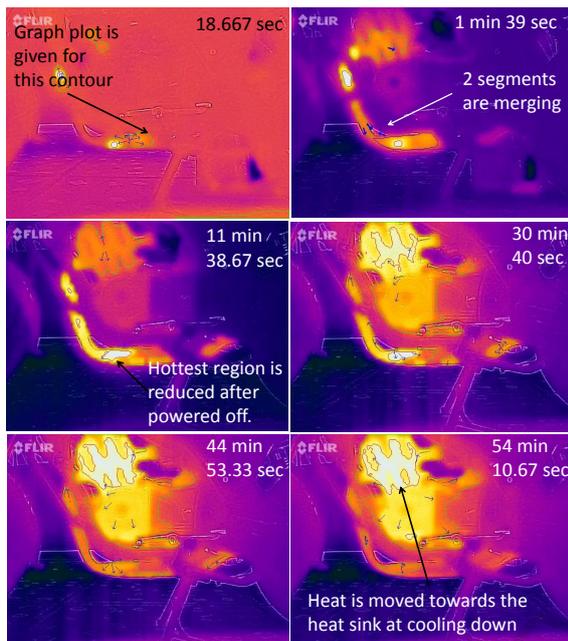
Figure 6: Motor Bike data set.

4.4 Key Frame

Transfer of heat is the flow of thermal energy between physical components in a system, whereby the internal energy of the system gets changed. In a system, the rate of heat transfer between two components or points, depends on the temperature difference between the respective components or points and the intervening medium of heat transfer. The direction of such flow of thermal energy is from higher temperature to lower temperature and the governing physics of the process is known as the second law of thermodynamics. Thermal equilibrium is reached when the bodies involved in heat transfer and the surrounding reach the same temperature. The three fundamental modes of heat transfer are conduction, convection and radiation. Heat transfer will result in the increase in entropy of the collection of systems. So the heat propagation on machine is dynamic process and rate varies with time. We found very minor heat changes between two consecutive frames when we captured continuous video through FLIR ONE. Therefore calculation is performed with reference of key frames rather every consecutive frames. Key frames are chosen after certain intervals. All other frames are compared with last stored key frame.

5 HEAT FLOW ANALYSIS

Analysis is performed in terms of comparing signatures and flow measurements between current and previous key frame. All measurements are performed in pixel unit. Therefore the changes are not possible in absolute unit rather in percentage changes. Area, perimeter and average intensity changes are recorded. Average intensity play an important role for identifying the event where changes in contour or shape are negligible but the region gets heated up slowly and uniformly with time.

Heat flow is measured by the changes of average Euclidean distances of each bucket. Every bucket are aligned with specific direction, so any changes of Euclidean distance on a bucket represent a change of heat towards the aligned direction.

Algorithm 2: Thermal Flow Measurement.

1: **procedure** HEATFLOW
2:     *loop*: [for all Buckets $\in$ segment]
3:     $J_{Dist} \leftarrow 0$
4:     *loop*: [for all point J $\in$ Bucket]
5:     $Y_{diff} \leftarrow (J.y - C.y)$
6:     $X_{diff} \leftarrow (J.x - C.x)$
7:     $\theta \leftarrow (\tan^{-1} \frac{Y_{diff}}{X_{diff}})$
8:     $J_{Dist} \leftarrow J_{Dist} + \sqrt{X_{diff}^2 + Y_{diff}^2}$
9:     *end loop*
10:     $HeatFlow_b \leftarrow \frac{J_{Dist}}{N}$ [N is the total number of points in the bucket]
11:     *end loop*

---

6 EXPERIMENTS

In this section we evaluate our presented system by testing on machine and prove that our system is capable to measure heat flow from thermal image. We analyse our proposed model using real thermal images of running machines that generate heat. In our experiments we concentrate to capture long duration videos to analyse the heat spread over time. Proposed system is implemented on personal computer but it can directly be ported on any smartphone using only cpu. A demo video is uploaded at https://youtu.be/Slj3Xw3XDsg to demonstrate the capability of the proposed system.

6.1 Evaluation with Bike engine

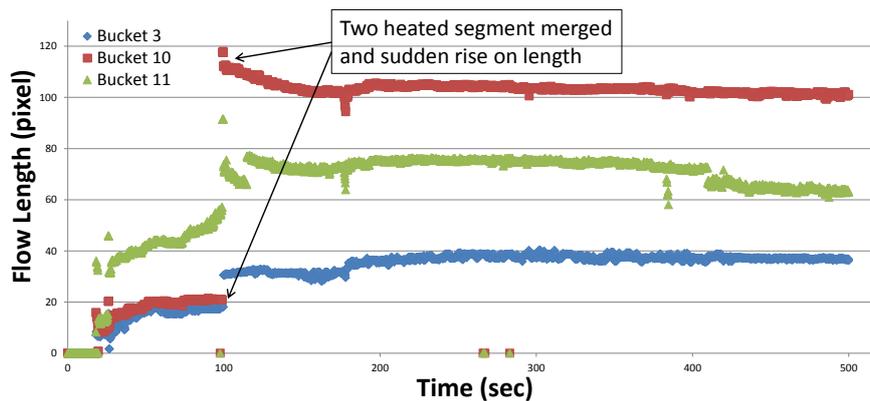We measured thermal flow on motor bike engine. The bike was powered on for 227 sec and heat flow of

Figure 7: Thermal flows for 3 buckets for bike data.

smoke pipe is measured for 55 min 13 sec. Detected contour and measured flow directions are presented in Fig. 6. Calculated thermal flow for 3 buckets for 500 sec are presented on Fig. 7. Bucket 10 shows a sudden increment at 99.16 sec which is the result of merging two contours towards that direction. Heat is flowed from engine towards heat sink after switching off the engine (shown on Fig. 6), which could be an indicative for predictive maintenance.

6.2 Evaluation with Heated Iron

Figure 8 represents snapshots of images with detected contours thermal flows of a house hold pressing iron. The entire test duration is 40 min 49 sec. Heat levels are incremented multiple times which is immediately detected on the flow measurement. Spreading of heat from heated iron body to the air is also detected by heat flow directions (22 min 39.17 sec onwards) and uniform heat distribution is also measured after the iron is cooled down by average intensity and area.

7 CONCLUSION

We presented a cost effective system for heat flow analysis of machines in autonomous and unobtrusive way with the use of FLIR ONE imaging camera. The system captures thermal video and track heated regions continuously. Heat flow analysis presented in the form of percentage changes of heat in all direction. Proposed method is capable of detecting and measuring any sudden heat flow, uniform heating from any heat source, merging of multiple heat sources etc. Presented results showed the above mentioned measurements and verify the claims. The system is tested with many machines that are commonly available in houses and results from two different tests

are presented. The measured attributes are expected to help for predictive maintenance for industrial machines and tolls that generates heat. Predictive or preventive maintenance for industrial machines are taken as the future scope of the work.

REFERENCES

Al-Habaibeh, A. and Robert, P. (2003). An autonomous low-cost infrared system for the on-line monitoring of manufacturing processes using novelty detection. In *International Journal of Advanced Manufacturing Technology*.

Alvy, R. S. (1978). Color gamut transform pairs. In *Special Interest Group on Graphics and Interactive Techniques (SIGGRAPH'78)*.

ASHISH and VIJAY (2014). Review on thermal image processing tecniques for machine condition monitoring. In *International Journal*.

Bagavathiappan, S., Saravanan, T., Philip, J., Jayakumar, T., Raj, B., Karunanithi, R., Panicker, T. M. R., Korath, M. P., and Jagadeesan, K. (2009). Infrared thermal imaging for detection of peripheral vascular disorders. In *Journal of Medical Physics*.

Clough, D., Fletcher, S., Longstaff, A. P., and Willoughby, P. (2012). Thermal analysis for condition monitoring of machine tool spindles. In *Journal of Physics: Conference Series*.

Deshpande, P., Reddy, V. R., Saha, A., Vaiapury, K., Dewangan, K., and Dasgupta, R. (2015). A next generation mobile robot with multi-mode sense of 3d perception. In *IEEE International Conference on Advanced Robotics (ICAR)*.

Eftekhari, M., Moallem, M., Sadri, S., and Hsieh, M. (2013). A novel indicator of stator winding inter-turn fault in induction motor using infrared thermal imaging. In *Infrared Physics and Technology*.

Kaczmarek, M. and Ruminski, J. (2009). Thermal imaging of skin temperature distribution during and after cooling: In-vitro experiments. In *4th European Confer-*

ence of the International Federation for Medical and Biological Engineering.

Omar, O., Jason, C., and Avideh, Z. (2014). Automatic generation of 3d thermal maps of building interiors. In *ASHRAE Trans*.

Pal, A., Dasgupta, R., Saha, A., and Nandi, B. (2016). Human-like sensing for robotic remote inspection and analytics. In *Wireless Personal Communications: An International Journal*.

Rafael, C. G. and Richard, E. W. (2006). *Digital Image Processing*. Prentice-Hall, Upper Saddle River, NJ, USA, 3rd edition.

Rajoub, B. A. and Zwiggelaar, R. (2014). Thermal facial analysis for deception detection. In *IEEE Trans. on Information Forensics and Security*.

Rangel, J., Soldan, S., and Kroll, A. (2014). 3d thermal imaging: Fusion of thermography and depth cameras. In *15th International Conference on Quantitative InfraRed Thermography*.

Saha, A., Dewangan, K., and Dasgupta, R. (2016). 3d thermal monitoring and measurement using smartphone and ir thermal sensor. In *11th Joint Conference on Computer Vision, Imaging and Computer Graphics Theory and Applications*.

Satoshi, S. and KeiichiA, A. (1985). Topological structural analysis of digitized binary images by border following. In *Computer Vision, Graphics, and Image Processing (CVGIP'85)*.

Starman, S. and Matz, V. (2011). Automated system for crack detection using infrared thermographic testing. In *Journal of Physics: Conference Series*.

Vidas, S., Moghadam, P., and Bosse, M. (2013). 3d thermal mapping of building interiors using an rgb-d and thermal camera. In *IEEE International Conference on Robotics and Automation (ICRA'13)*.

Weinmann, M., Leitloff, J., Hoegner, L., Jutzi, B., Stilla, U., and Hinz, S. (2014). Thermal 3d mapping for object detection in dynamic scenes. In *ISPRS Annals of the Photogrammetry, Remote Sensing and Spatial Information Sciences*.
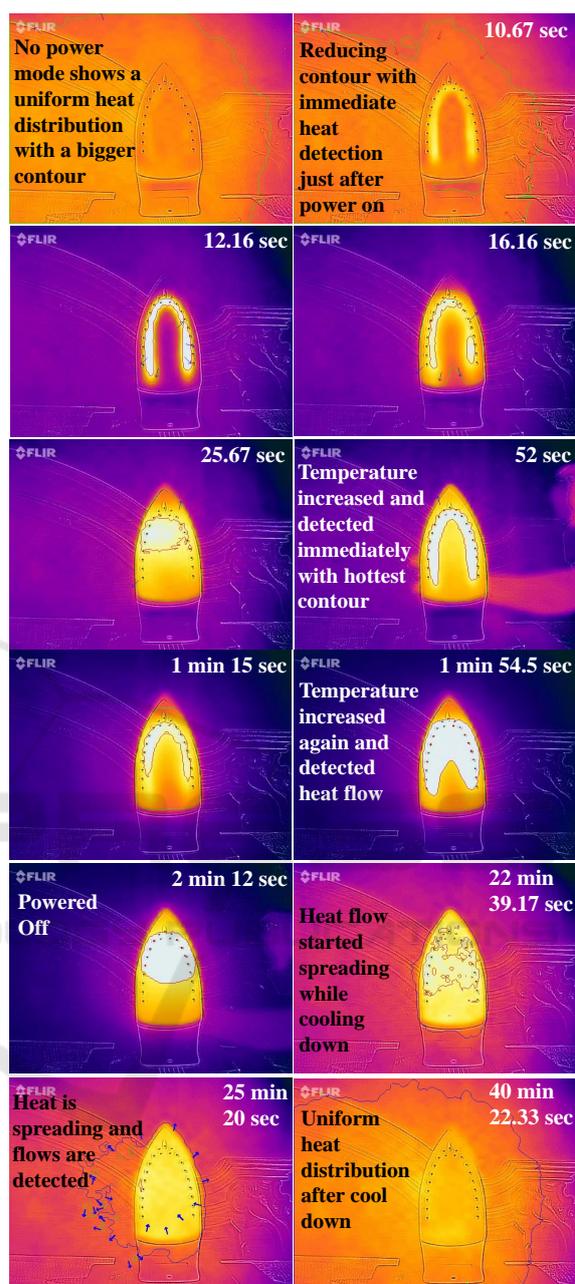
Figure 8: Iron data set.